

ARTICLE OPEN

Accessible quantification of multiparticle entanglement

Marco Cianciaruso^{1,2}, Thomas R Bromley^{1,2} and Gerardo Adesso¹

Entanglement is a key ingredient for quantum technologies and a fundamental signature of quantumness in a broad range of phenomena encompassing many-body physics, thermodynamics, cosmology and life sciences. For arbitrary multiparticle systems, entanglement quantification typically involves nontrivial optimisation problems, and it may require demanding tomographical techniques. Here, we develop an experimentally feasible approach to the evaluation of geometric measures of multiparticle entanglement. Our framework provides analytical results for particular classes of mixed states of N qubits, and computable lower bounds to global, partial, or genuine multiparticle entanglement of any general state. For global and partial entanglement, useful bounds are obtained with minimum effort, requiring local measurements in just three settings for any N . For genuine entanglement, a number of measurements scaling linearly with N are required. We demonstrate the power of our approach to estimate and quantify different types of multiparticle entanglement in a variety of N -qubit states useful for quantum information processing and recently engineered in laboratories with quantum optics and trapped ion setups.

npj Quantum Information (2016) 2, 16030; doi:10.1038/npjqi.2016.30; published online 18 October 2016

INTRODUCTION

The fascination with quantum entanglement has evolved over the last eight decades, from the realm of philosophical debate¹ to a very concrete recognition of its resource role in a range of applied sciences.^{2,3} Although considerable progress has been achieved in the detection of entanglement,^{4–12} its experimentally accessible quantification remains an open problem for any real implementation of an entangled system.^{13–23} Quantifying entanglement is yet necessary to gauge precisely the quantum enhancement in information processing and computation,^{2,3,24} and to pin down exactly how much a physical or biological system under observation departs from an essentially classical behaviour.²⁵ This is especially relevant in the case of complex, multiparticle systems, for which only quite recently have notable advances been reported on the control of entanglement.^{26–29}

An intuitive framework for quantifying the degree of multiparticle entanglement relies on a geometric perspective.^{30–32} Within this approach, one first identifies a hierarchy of non-entangled multiparticle states, also referred to as M -separable states for $2 \leq M \leq N$, where N is the number of particles composing the quantum system of interest; see Figure 1. Introducing then a distance functional D with respect to the natural properties of contractivity under quantum operations and joint convexity (see Materials and Methods),³³ the quantity E_M^D defined as

$$E_M^D(\rho) = \inf_{\varsigma \text{ } M\text{-separable}} D(\rho, \varsigma), \quad (1)$$

is a valid geometric measure of (M -inseparable) multiparticle entanglement in the state ρ .

Some special cases are prominent in this hierarchy. For $M=N$, the distance from N -separable (also known as fully separable) states defines the *global* multiparticle entanglement E_N^D , which accounts for any form of entanglement distributed among

two or more of the N particles. Geometric measures of global entanglement have been successfully employed to characterise quantum phase transitions in many-body systems³⁴ and directly assess the usefulness of initial states for Grover's search algorithms.³⁵ On the other extreme of the hierarchy, for $M=2$, the distance from two-separable (also known as biseparable) states defines instead the genuine multiparticle entanglement E_2^D , which quantifies the entanglement shared by all the N particles, that is the highest degree of inseparability. Genuine multiparticle entanglement is an essential ingredient for quantum technologies including multiuser quantum cryptography,³⁶ quantum metrology³⁷ and measurement-based quantum computation.³⁸ Finally, for any intermediate M , we can refer to E_M^D as *partial* multiparticle entanglement. The presence of partial entanglement is relevant in quantum informational tasks such as quantum secret sharing¹⁰ and may have a relevant role in biological phenomena.^{25,39} Probing and quantifying different types of entanglement can shed light on which nonclassical features of a mixed multiparticle state are necessary for quantum-enhanced performance in specific tasks⁷ and can guide the understanding of the emergence of classicality in multiparticle quantum systems of increasing complexity.⁴⁰

The quantitative amount of multiparticle entanglement, be it global or genuine (or any intermediate type), has an intuitive operational meaning when adopting the geometric approach. Namely, E_M^D measures how distinguishable a given state ρ is from the closest M -separable state. Given some widely adopted metrics, such a distinguishability is directly connected to the usefulness of ρ for quantum information protocols relying on multiparticle entanglement. For instance, the trace distance of entanglement is operationally related to the minimum probability of error in the discrimination between ρ and any M -separable state with a single measurement.³³ Furthermore, the geometric entanglement with respect to relative entropy or Bures distance sets quantitative

¹Centre for the Mathematics and Theoretical Physics of Quantum Non-equilibrium Systems, School of Mathematical Sciences, The University of Nottingham, University Park, Nottingham NG7 2RD, UK.

Correspondence: M Cianciaruso (cianciaruso.marco@gmail.com) TR Bromley (thomas.r.bromley@gmail.com) or G Adesso (gerardo.adesso@nottingham.ac.uk)

²These authors contributed equally to this work.

Received 13 May 2016; revised 10 July 2016; accepted 28 August 2016

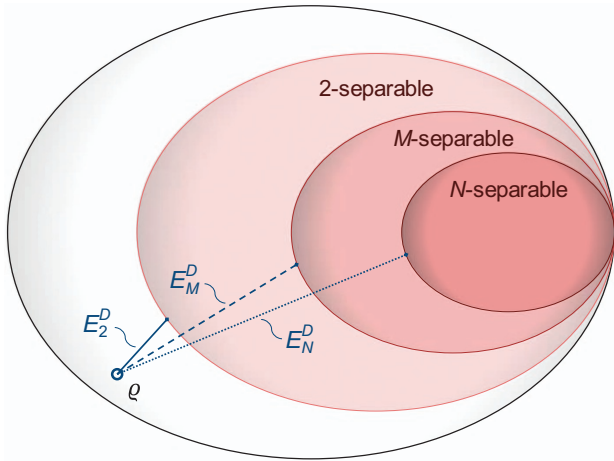


Figure 1. Geometric picture of multiparticle entanglement in a quantum system of N particles. Each red-shaded convex set contains M -separable states (for $2 \leq M \leq N$), which can be defined as follows. The set of pure M -separable states is given by the union of the sets of tensor products $|\Psi_M\rangle = \otimes_{k=1}^M |\psi^{(k)}\rangle$ of pure states $|\psi^{(k)}\rangle$, with respect to any partition of the N particles into M subsystems $k=1, \dots, M$; the set of general (mixed) M -separable states is then formed by all convex mixtures of pure M -separable states, where each term in the mixture may be factorised with respect to a different multipartition. This provides a partition-independent classification of separability (see also the Supplementary Material). For any M , the multiparticle entanglement measure E_M^D of a state ρ is defined as the minimum distance, with respect to a contractive and jointly convex distance functional D , from the set of M -separable states. We refer to the case $M=N$ (dotted line) as global entanglement, the case $M=2$ (solid line) as genuine entanglement and any intermediate case (dashed line) as partial entanglement, as detailed in the main text.

bounds on the number of orthogonal states that can be discriminated by local operations and classical communication (LOCC).⁴¹ The geometric entanglement based on infidelity³¹ (monotonically related to Bures distance) has also a dual interpretation based on the convex roof construction;⁴² that is, it quantifies the minimum price (in units of pure-state entanglement) that has to be spent on average to create a given density matrix ρ as a statistical mixture of pure states.

It is therefore clear that finding the minimum in Equation (1), and hence evaluating geometric measures of multiparticle entanglement defined by meaningful distances, is a central challenge to benchmark quantum technologies. However, obtaining such a solution for general multiparticle states is in principle a formidable problem. Even if possible, there would remain major challenges for experimental evaluation, which would in general require a complete reconstruction of the state through full tomography. For multiparticle states of any reasonable number of qubits, full state tomography places significant demands on experimental resources, and it is thus highly desirable to provide quantitative guarantees on the geometric multiparticle entanglement present in a state, via nontrivial lower bounds, in an experimentally accessible way.^{13–23}

Here we provide substantial advances towards addressing this problem in a general fashion. We identify a general framework for the provision of experimentally friendly quantitative guarantees on the geometric multiparticle entanglement present in a state. This approach consists of:

- (1) Choosing a set of reference states: find a restricted family of N -qubit states with the property that *any* state may be mapped into this family through a fixed procedure of single-qubit LOCC. This reference family should be simple to

characterise, and can be chosen from experimental or theoretical considerations.

- (2) Identifying M -separable reference states: Apply the fixed LOCC procedure to the general set of M -separable states, hence identifying the subset of M -separable states within the reference family.
- (3) Calculating E_M^D for the reference states: solve the optimisation problem for the geometric entanglement of reference states. This is markedly simplified by using the properties of contractivity and joint convexity, that hold for any distance functional D defining a valid entanglement measure, and imply in particular that one of the closest M -separable states to any reference state is to be found itself within the reference family.
- (4) Deriving optimised lower bounds for any state: exploit the freedom to apply single-qubit unitaries to any N -qubit state ρ in order to find the corresponding reference state with the highest geometric entanglement, providing an optimised lower bound to $E_M^D(\rho)$.

This process presents a versatile and comprehensive approach to obtain lower bounds on geometric multiparticle entanglement measures according to any valid distance. While building on some previously utilised methods for steps (1)^{13–16} and (4)^{13,15,16} it introduces novel techniques in steps (2) and most importantly (3), which are crucial for completing the framework and making it effective in practice (see e.g., Appendix C, D, E and F of the Supplementary Material).

To illustrate the power of our approach, we focus initially on a reference family of mixed states ϖ of N qubits, that we label \mathcal{M}_N^3 states, which form a subset of the class of states having all maximally mixed marginals. This family includes maximally entangled Bell states of two qubits and their mixtures, as well as multiparticle bound entangled states.^{43–46} For any N , these states are completely specified by three easily measurable quantities, given by the correlation functions $c_j = \langle \sigma_j^{\otimes N} \rangle$, where $\{\sigma_j\}_{j=1,2,3}$ are the Pauli matrices. In the following we show how every entanglement monotone E_M^D can be evaluated exactly for any even N on these states, by revealing an intuitive geometric picture common to all valid distances D . For odd N , the results are distance-dependent; we show nonetheless that E_M^D can still be evaluated exactly if D denotes the trace distance. The results are nontrivial for all $M > \lceil N/2 \rceil$ in the hierarchy of Figure 1. A central observation, in line with the general framework, is that an arbitrary state of N qubits can be transformed into an \mathcal{M}_N^3 state by an LOCC procedure, which cannot increase entanglement by definition. This implies that our exact formulae readily provide practical lower bounds to the degree of global and partial multiparticle entanglement in completely general states. Importantly, the bounds are obtained by measuring only the three correlation functions $\{c_j\}$ for any number of qubits, and can be further improved by adjusting the local measurement basis (see Figure 2 for an illustration).

Furthermore, we discuss how our results can be extended to allow for the quantitative estimation of genuine multiparticle entanglement as well, at the cost of performing extra measurements. As \mathcal{M}_N^3 states are always biseparable, we must consider a different reference family. We focus on the class of N -qubit states obtained as mixtures of Greenberger–Horne–Zeilinger (GHZ) states,^{5,47} the latter being central resources for quantum communication and estimation; this class of states depends on $2^N - 1$ real parameters. We calculate exactly distance-based measures of genuine multiparticle entanglement E_2^D for these states, for every valid D . Once more, these analytical results provide lower bounds to geometric measures of genuine entanglement for any general state of N qubits, obtainable

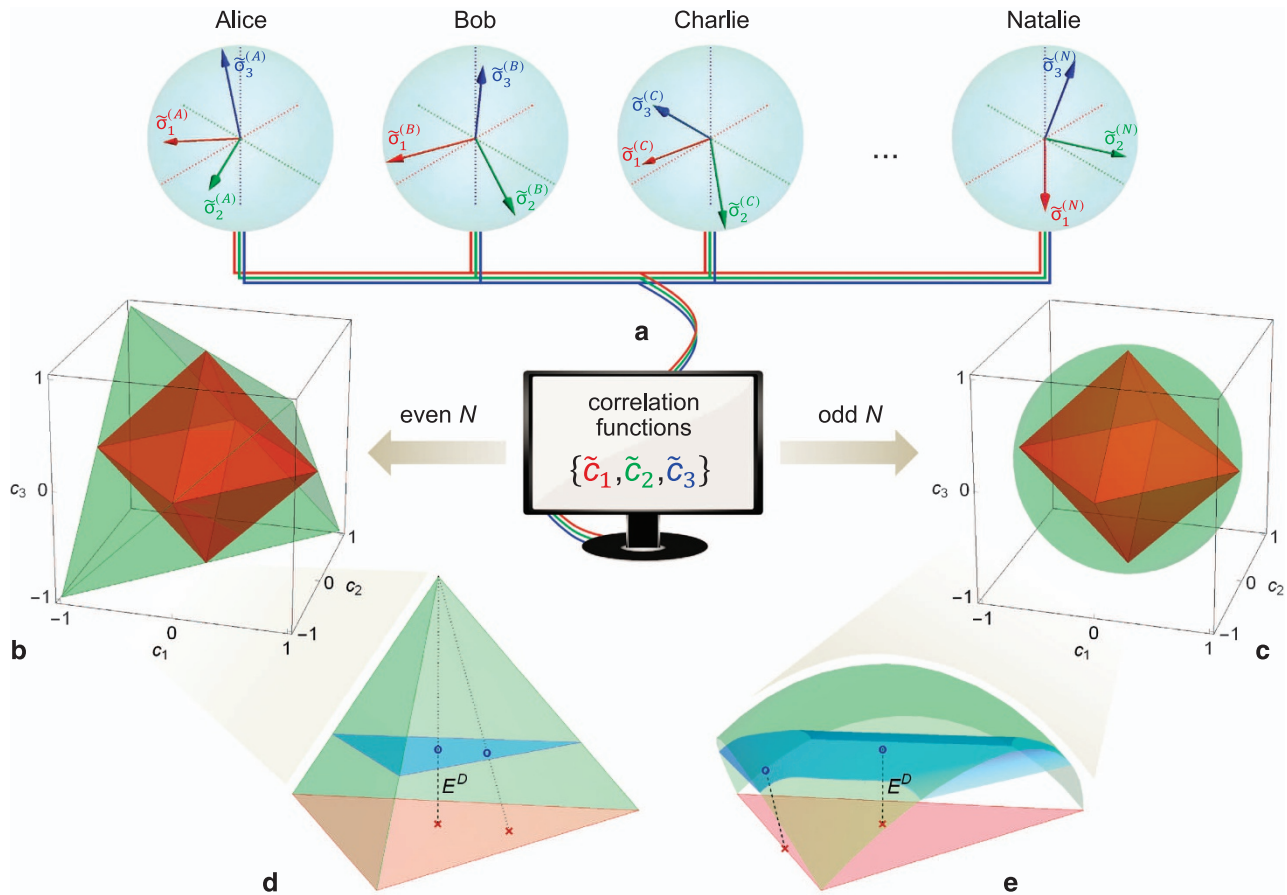


Figure 2. Experimentally friendly protocol to quantify global and partial N -particle entanglement. *Top row: (a)* A state ρ of N qubits is shared by N parties, named Alice, Bob, Charlie, ..., Natalie. Each party, labelled by $a = A, \dots, N$, locally measures her or his qubit in three orthogonal directions $\{\tilde{\sigma}_j^{(a)}\}$, with $j = 1, 2, 3$, indicated by the solid arrows. If the shared state ρ is completely unknown, a standard choice can be to measure the three canonical Pauli operators for all the qubits (corresponding to the directions of the dashed axes); if instead some partial information on ρ is available, the measurement directions can be optimised *a priori*. Once all the data are collected, the N parties communicate classically to construct the three correlation functions $\{\tilde{c}_j\}$, with $\tilde{c}_j = \langle \otimes_a \tilde{\sigma}_j^{(a)} \rangle$. *Middle row: (b)* For even N , \mathcal{M}_N^3 states fill the tetrahedron with vertices $\{1, (-1)^{N/2}, 1\}$, $\{-1, -(-1)^{N/2}, 1\}$, $\{1, -(-1)^{N/2}, -1\}$ and $\{-1, (-1)^{N/2}, -1\}$. *(c)* For odd N , they are instead contained in the unit Bloch ball. For any $M > \lceil N/2 \rceil$, M -separable \mathcal{M}_N^3 states are confined to the octahedron with vertices $\{\pm 1, 0, 0\}$, $\{0, \pm 1, 0\}$ and $\{0, 0, \pm 1\}$, illustrated in red in both panels; conversely, for $M \leq \lceil N/2 \rceil$, all \mathcal{M}_N^3 states are M -separable. *Bottom row: (d)* a corner of the tetrahedron for even N and *(e)* a sector of the unit sphere for odd N , opposing a face of the octahedron of M -separable \mathcal{M}_N^3 states (for $M > \lceil N/2 \rceil$). Instances of inseparable \mathcal{M}_N^3 states are indicated by blue circles, and their closest M -separable states by red crosses. The cyan surfaces in each of the two bottom panels contain states with equal global and partial multiparticle entanglement E_M^D , which we compute exactly. The results are valid for any contractive and jointly convex D in the even N case, and for the trace distance in the odd N case. The entanglement of an \mathcal{M}_N^3 state with correlation functions $\{\tilde{c}_1, \tilde{c}_2, \tilde{c}_3\}$ provides an analytical lower bound for the entanglement of any N -qubit state with the same correlation functions, such as the state ρ initially shared by the N parties in *a*. The bound is effective for the most relevant families of N -qubit states in theoretical and experimental investigations of quantum information processing, as we show in this article.

experimentally in this case by performing at least $N+1$ local measurements.⁴⁸

We demonstrate that our results provide overall accessible quantitative assessments of global, partial and genuine multiparticle entanglement in a variety of noisy states produced in recent experiments,^{40,44,49–52} going beyond mere detection,^{4–12} yet with a significantly reduced experimental overhead. Compared with some recent complementary approaches to the quantification of multiparticle entanglement,^{13–23} we find that our results, obtained via the general quantitative framework discussed above, fare surprisingly well in their efficiency and versatility despite the

minimal experimental requirements (see Table 1 for an in-depth comparison).

RESULTS

Global and partial multiparticle entanglement

We begin by choosing as our reference family the set of N -qubit \mathcal{M}_N^3 states. An \mathcal{M}_N^3 state is defined as $\varpi = \frac{1}{2^N} (\mathbb{I}^{\otimes N} + \sum_{j=1}^3 c_j \sigma_j^{\otimes N})$, where \mathbb{I} is the 2×2 identity matrix. These states are invariant under permutations of any pair of qubits and enjoy a nice

Table 1. A comparison of relevant literature on experimentally friendly quantification of multiparticle entanglement (based on accessible lower bounds)

Reference	Experimental friendliness	Computational friendliness	M-inseparability quantified	Entanglement measure
22,23	Variable	Optimisation required	$2 \leq M \leq N$	Any convex and continuous measure
21	$O(2^N)$	Optimisation required	2	Genuine multiparticle concurrence
19,20	$O(N)$	Closed formula	2	Robustness of entanglement
18	$O(N)$	Closed formula	2	Genuine multiparticle concurrence
17	$O(N)$	Closed formula	2	Genuine multiparticle concurrence
15,16	$O(N)$	Closed formula	2	Polynomial invariant (three-tangle)
14	$O(N)$	Closed formula	2	Genuine multiparticle negativity
13	$O(N)$	Closed formula	$2 \leq M \leq N$	Infidelity-based geometric measure
[*] (GHZ-diagonal set)	$O(N)$	Closed formula	2	All distance-based measures
[*] (\mathcal{M}_N^3 set)	3	Closed formula	$\lceil N/2 \rceil < M \leq N$	All distance-based measures

For each reference, we give the experimental friendliness, in terms of the number of local measurement settings required, and also the computational friendliness. The levels of M -inseparability quantified are given, along with the entanglement measures to which each work applies; [*] refers to this paper.

Table 2. Analytical expression of global and partial multiparticle entanglement E_M^D for \mathcal{M}_N^3 states of an even number N of qubits as defined by Equation (2), for representative choices of the distance D

Distance D	$D(\rho, \varsigma)$	$f_D(h_\varpi)$
Relative entropy D_{RE}	$\text{Tr}[\rho(\log_2 \rho - \log_2 \varsigma)]$	$\frac{1}{2}[(1-h_\varpi)\log_2(1-h_\varpi) + (1+h_\varpi)\log_2(1+h_\varpi)]$
Trace D_{Tr}	$\frac{1}{2} \text{Tr}[\rho - \varsigma] $	$\frac{1}{2}h_\varpi$
Infidelity D_F	$1 - [\text{Tr}(\sqrt{\sqrt{\varsigma}\rho\sqrt{\varsigma}})]^2$	$\frac{1}{2}\left(1 - \sqrt{1-h_\varpi^2}\right)$
Squared Bures D_B	$2[1 - \text{Tr}(\sqrt{\sqrt{\varsigma}\rho\sqrt{\varsigma}})]$	$2 - \sqrt{1-h_\varpi} - \sqrt{1+h_\varpi}$
Squared Hellinger D_H	$2[1 - \text{Tr}(\sqrt{\rho\varsigma})]$	$2 - \sqrt{1-h_\varpi} - \sqrt{1+h_\varpi}$

geometrical representation in the space of the three correlation functions c_j , corresponding to a tetrahedron for even N and to the unit ball for odd N , as depicted in Figure 2. We can then characterise the subset of M -separable \mathcal{M}_N^3 states for any N . We find that, if $M > \lceil N/2 \rceil$, then the M -separable \mathcal{M}_N^3 states fill a subset corresponding to an octahedron in the space of the correlation functions (Figure 2). When $M \leq \lceil N/2 \rceil$, all \mathcal{M}_N^3 states are instead M -separable. The proofs are deferred to the Supplementary Material.

We can now tackle the quantification of global and partial multiparticle entanglement in these states; for the latter, we will always focus on the nontrivial case $M > \lceil N/2 \rceil$ throughout this section. First, we observe that the closest M -separable state ς_ϖ to an \mathcal{M}_N^3 state ϖ , which solves the optimisation in Equation (1), can always be found within the subset of M -separable \mathcal{M}_N^3 states, yielding a considerable simplification of the general problem. To find the exact form of ς_ϖ and consequently of $E_M^D(\varpi)$, we approach the cases of even and odd N separately.

For even N , we prove that there exists a unique solution to the minimisation in Equation (1), independent of the specific choice of contractive and jointly convex distance D . Namely, the closest M -separable state ς_ϖ is on the face of the octahedron bounding the corner of the tetrahedron in which ϖ is located, and is identified by the intersection of such octahedron face with the line connecting ϖ to the vertex of the tetrahedron corner, as depicted in Figure 2d. It follows that, for any nontrivial M , valid D and even N , the multiparticle entanglement $E_M^D(\varpi^{\{c_j\}})$ of an \mathcal{M}_N^3 state $\varpi^{\{c_j\}}$ with correlation functions $\{c_j\}$ is only a monotonically increasing function of the Euclidean distance between the point of coordinates $\{c_j\}$ and the closest octahedron face, which is in turn proportional to $h_\varpi = \frac{1}{2}(\sum_{j=1}^3 |c_j| - 1)$ (notice that h_ϖ equals the bipartite measure known as concurrence for $N=2$ (refs 24,53)). We have then a closed formula for any valid geometric measure of

global and partial multiparticle entanglement on an arbitrary \mathcal{M}_N^3 state $\varpi^{\{c_j\}}$ with even N , given by

$$E_M^D(\varpi^{\{c_j\}}) = \begin{cases} 0, & h_\varpi \leq 0 \text{ (or } M \leq N/2\text{)}; \\ f_D(h_\varpi), & \text{otherwise,} \end{cases} \quad (2)$$

where f_D denotes a monotonically increasing function whose explicit form is specific to each distance D . In Table 2, we present the expression of f_D for relevant distances in quantum information theory.

For odd N , the closest M -separable state ς_ϖ to any \mathcal{M}_N^3 state ϖ is still independent of (any nontrivial) M . However, different choices of D in Equation (1) are minimised by different states ς_ϖ . We focus on the important but notoriously hard-to-evaluate case of the trace distance $D_{Tr}(\varpi, \varsigma)$ (Table 2). In the representation of Figure 2c, the trace distance amounts to half the Euclidean distance on the unit ball. It follows that the closest M -separable state ς_ϖ to ϖ is the Euclidean orthogonal projection onto the boundary of the octahedron, see Figure 2e. We can then get a closed formula for the trace distance measure of global and partial multiparticle entanglement $E_M^{D_{Tr}}(\varpi^{\{c_j\}})$ of an arbitrary \mathcal{M}_N^3 state $\varpi^{\{c_j\}}$ with odd N as well, given by

$$E_M^{D_{Tr}}(\varpi^{\{c_j\}}) = \begin{cases} 0, & h_\varpi \leq 0 \text{ (or } M \leq \lceil N/2 \rceil\text{)}; \\ \frac{h_\varpi}{\sqrt{3}}, & 0 < h_\varpi \leq 3|c_j|/2 \quad \forall j; \\ \min_j \frac{1}{2} \sqrt{|c_j|^2 + \frac{1}{2}(2h_\varpi - |c_j|)^2}, & \text{otherwise.} \end{cases} \quad (3)$$

The usefulness of the just-derived analytical results for multiparticle entanglement is not limited to the \mathcal{M}_N^3 states. In accordance with our general framework, a crucial observation is that the \mathcal{M}_N^3 states are extremal among all quantum states with given correlation functions $\{c_j\}$. Specifically, any general state ρ of N qubits can be transformed into an \mathcal{M}_N^3 state with the same $\{c_j\}$

Table 3. Applications of our framework to construct accessible lower bounds on global and partial (M -inseparable) multiparticle entanglement (which are nonzero for any $M > \lceil N/2 \rceil$ when $\sum_j |\tilde{c}_j| > 1$), for the families of N -qubit states listed as follows

N	State	$\{\tilde{c}_1, \tilde{c}_2, \tilde{c}_3\}$	$\sum_{j=1}^3 \tilde{c}_j $	$\{\theta, \psi, \phi\}$
$N=3$	$ \text{GHZ}^{(3)}\rangle$	$\left\{-\sqrt{\frac{8}{27}}, \sqrt{\frac{8}{27}}, -\sqrt{\frac{8}{27}}\right\}$	$2\sqrt{\frac{2}{3}}$	$\left\{\cos^{-1}\left(\frac{1}{\sqrt{3}}\right), \frac{5\pi}{30}, \frac{\pi}{4}\right\}$
	$ \text{W}^{(3)}\rangle$	$\left\{\frac{1}{\sqrt{3}}, -\frac{1}{\sqrt{3}}, \frac{1}{\sqrt{3}}\right\}$	$\sqrt{3}$	$\left\{\cos^{-1}\left(\frac{1}{\sqrt{3}}\right), 0, \frac{\pi}{4}\right\}$
$N=4$	$ \text{GHZ}^{(4)}\rangle$	$\{1, 1, 1\}$	3	$\{0, 0, 0\}$
	$ \text{W}^{(4)}\rangle$	$\left\{\frac{5}{9}, \frac{5}{9}, \frac{5}{9}\right\}$	$\frac{5}{3}$	$\left\{\cos^{-1}\left(\frac{1}{\sqrt{3}}\right), 0, \frac{\pi}{4}\right\}$
	$\rho_{\text{Wei}}^{(4)}(x)$	$\{x, x, 2x-1\}$	$2x + 2x-1 $	$\{0, 0, 0\}$
	$ \text{C}_1^{(4)}\rangle$	$\{1, 1, 1\}$	3	*
	$ \text{C}_2^{(4)}\rangle$	$\{1, 1, 1\}$	3	$\{\frac{\pi}{4}, 0, 0\}$
	$ \text{D}_2^{(4)}\rangle$	$\{1, 1, 1\}$	3	$\{0, 0, 0\}$
	$ \psi^{(4)}\rangle$	$\{1, 1, 1\}$	3	$\{0, 0, 0\}$
	$\rho_S^{(4)}$	$\{1, 1, 1\}$	3	$\{0, 0, 0\}$
$N=5$	$ \text{GHZ}^{(5)}\rangle$	$\left\{\frac{1}{\sqrt{2}}, \frac{1}{\sqrt{2}}, 0\right\}$	$\sqrt{2}$	$\{0, \frac{\pi}{40}, \frac{\pi}{40}\}$
	$ \text{W}^{(5)}\rangle$	$\left\{\frac{7}{9\sqrt{3}}, -\frac{7}{9\sqrt{3}}, \frac{7}{9\sqrt{3}}\right\}$	$\frac{7}{3\sqrt{3}}$	$\left\{\cos^{-1}\left(\frac{1}{\sqrt{3}}\right), 0, \frac{\pi}{4}\right\}$
	$\rho_{\text{Wei}}^{(5)}(x)$	$\left\{\frac{x}{\sqrt{2}}, \frac{x}{\sqrt{2}}, 0\right\}$	$\sqrt{2}x$	$\{0, \frac{\pi}{40}, \frac{\pi}{40}\}$
	$ \text{C}_1^{(5)}\rangle$	$\left\{\frac{1}{2}, \frac{1}{2}, \frac{1}{2}\right\}$	$\frac{3}{2}$	*
$N=6$	$ \text{GHZ}^{(6)}\rangle$	$\{1, -1, 1\}$	3	$\{0, 0, 0\}$
	$\rho_{\text{Wei}}^{(6)}(x)$	$\{x, -x, 2x-1\}$	$2x + 2x-1 $	$\{0, 0, 0\}$
	$ \text{C}_1^{(6)}\rangle$	$\{1, -1, 1\}$	3	*
	$ \text{C}_2^{(6)}\rangle$	$\{1, -1, 1\}$	3	*
	$ \text{D}_3^{(6)}\rangle$	$\{1, 1, -1\}$	3	$\{0, 0, 0\}$
	$\rho_S^{(6)}$	$\{-1, -1, -1\}$	3	$\{0, 0, 0\}$
$N=7$	$ \text{GHZ}^{(7)}\rangle$	$\left\{\frac{1}{\sqrt{2}}, -\frac{1}{\sqrt{2}}, 0\right\}$	$\sqrt{2}$	$\{0, \frac{\pi}{56}, \frac{\pi}{56}\}$
	$\rho_{\text{Wei}}^{(7)}(x)$	$\left\{\frac{x}{\sqrt{2}}, -\frac{x}{\sqrt{2}}, 0\right\}$	$\sqrt{2}x$	$\{0, \frac{\pi}{56}, \frac{\pi}{56}\}$
	$ \text{C}_1^{(7)}\rangle$	$\left\{\frac{1}{2}, -\frac{1}{2}, \frac{1}{2}\right\}$	$\frac{3}{2}$	*
$N=8$	$ \text{GHZ}^{(8)}\rangle$	$\{1, 1, 1\}$	3	$\{0, 0, 0\}$
	$\rho_{\text{Wei}}^{(8)}(x)$	$\{x, x, 2x-1\}$	$2x + 2x-1 $	$\{0, 0, 0\}$
	$ \text{C}_1^{(8)}\rangle$	$\{1, 1, 1\}$	3	*
	$ \text{D}_4^{(8)}\rangle$	$\{1, 1, 1\}$	3	$\{0, 0, 0\}$
	$\rho_S^{(8)}$	$\{1, 1, 1\}$	3	$\{0, 0, 0\}$

(i) N -qubit GHZ states⁴⁷ $|\text{GHZ}^{(N)}\rangle = \frac{1}{\sqrt{2}}(|00 \dots 00\rangle + |11 \dots 11\rangle)$ with $N \geq 3$. (ii) N -qubit W states⁵⁴ $|\text{W}^{(N)}\rangle = \frac{1}{\sqrt{N}}(|00 \dots 01\rangle + |00 \dots 10\rangle + \dots + |10 \dots 00\rangle)$, with $N \geq 3$. (iii) N -qubit Wei states^{55,56} $\rho_{\text{Wei}}^{(N)}(x) = x|\text{GHZ}^{(N)}\rangle\langle\text{GHZ}^{(N)}| + \frac{(1-x)}{2N} \sum_{k=1}^N (P_k + \bar{P}_k)$, where $N \geq 4$, $x \in [0, 1]$ and P_k is the projector onto the binary N -qubit representation of 2^{k-1} , whereas $\bar{P}_i = \sigma_1^{\otimes N} P_i \sigma_1^{\otimes N}$. (iv) N -qubit linear cluster states $|\text{C}_1^{(N)}\rangle$ corresponding to the N -vertex linear graph $\bullet - \bullet - \dots - \bullet$.^{14,38} (v) N -qubit rectangular cluster states $|\text{C}_2^{(N)}\rangle$ corresponding to the N -vertex ladder-type graph $\begin{array}{c} \bullet - \bullet - \dots - \bullet \\ | \quad | \quad \quad | \\ \bullet - \bullet - \dots - \bullet \end{array}$.^{38,57} (vi) N -qubit (symmetric) Dicke states $|\text{D}_k^{(N)}\rangle = \frac{1}{\sqrt{Z}} \sum_i \Pi_i \left(|0\rangle^{\otimes N-k} \otimes |1\rangle^{\otimes k} \right)$, which are superpositions of all states with k qubits in the excited state $|1\rangle$ and $N-k$ qubits in the ground state $|0\rangle$, with the symbol $\{\Pi_i(\cdot)\}_{i=1}^Z$ denoting all the $Z \equiv \binom{N}{k}$ distinct permutations of 0's and 1's; we focus on half-excited Dicke states, given by $k=N/2$ for any even N .^{51,52,58,66} (vii) 4-qubit singlet state⁶² $|\psi^{(4)}\rangle = \frac{1}{\sqrt{3}}[|0011\rangle + |1100\rangle - (|0101\rangle + |0110\rangle + |1001\rangle + |1010\rangle)]/2$. (viii) N -qubit generalised Smolin states^{43,46,68} $\rho_S^{(N)}$ for even $N \geq 4$, which are instances of \mathcal{M}_N^3 states with correlation triple $\{(-1)^{N/2}, (-1)^{N/2}, (-1)^{N/2}\}$, hence their entanglement quantification is exact. The asterisk indicates non-permutationally invariant states for which the optimisation of the bounds requires different angles for each qubit (not reported here). Notice that in the table we listed mostly pure states. In general, if the triple $\{\tilde{c}_j\}$ is optimal for a pure N -qubit state $|\Phi^{(N)}\rangle$, then for the mixed state $\rho^{(N)}(q) = q|\Phi^{(N)}\rangle\langle\Phi^{(N)}| + \frac{1-q}{2^N} \mathbb{I}^{\otimes N}$, obtained by mixing $|\Phi^{(N)}\rangle$ with white noise, one still gets nonzero lower bounds to global and partial entanglement for all $q > 1/\sum_{j=1}^3 |\tilde{c}_j|$, as shown in Figure 3 for some representative examples.

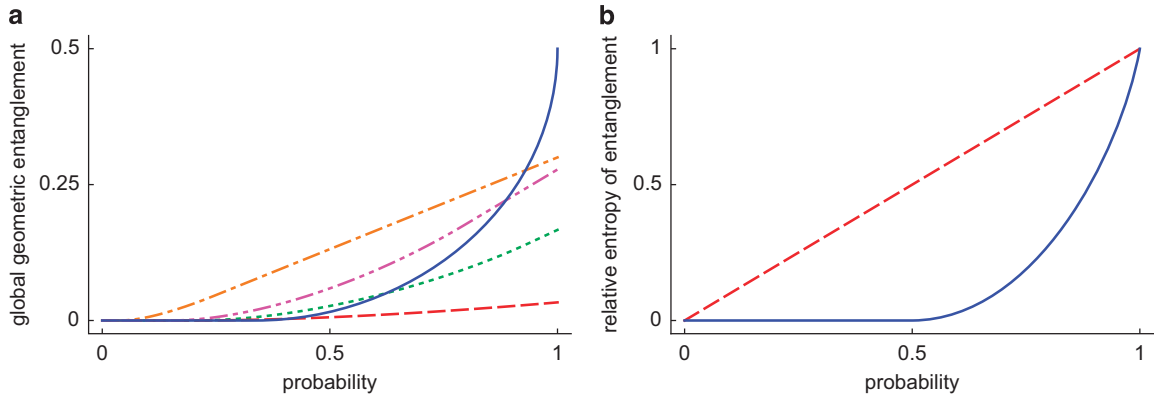


Figure 3. (a) Lower bounds to the global geometric entanglement E_N^{Df} based on infidelity for noisy versions of some N -qubit states (defined in the caption of Table 3), as functions of the probability q of obtaining the corresponding pure states. The non-solid lines refer to bounds obtained by the method of ref. 13 for: 4-qubit linear cluster state (green dotted), 6-qubit rectangular cluster state (red dashed), 6-qubit half-excited Dicke state (orange dot-dashed), 4-qubit singlet state (magenta dot-dot-dashed). The solid blue line corresponds to our bound based on \mathcal{M}_N^3 -fication for all the considered states, which is accessible by measuring only the three correlation functions $\tilde{c}_j = \langle \otimes_a \tilde{\sigma}_j^{(a)} \rangle$. (b) Relative entropy of multiparticle entanglement of N -qubit Wei states $\rho_{\text{Wei}}^{(N)}$ defined in Table 3, as a function of the probability x of obtaining a GHZ state. The dashed red line $E_N^{Df}(\rho_{\text{Wei}}^{(N)}) = x$ denotes the exact value of the global relative entropy of entanglement as computed in ref. 56. The solid blue line denotes our accessible lower bound, obtained by combining Equations (2) and (5) with the expressions in Tables 2 and 3, and given explicitly by $E_{N,\text{low}}^{Df}(\rho_{\text{Wei}}^{(N)}) = \log_2(2-2x) + x(\log_2(x) - \log_2(1-x))$ for $\frac{1}{2} < x \leq 1$, while it vanishes for $0 \leq x \leq \frac{1}{2}$. The bound becomes tight for $x = 1$, thus quantifying exactly the global multiparticle entanglement of pure GHZ states. We further show that our lower bound to global entanglement coincides with the exact genuine multiparticle entanglement of Wei states, $E_{N,\text{low}}^{Df}(\rho_{\text{Wei}}^{(N)}) = E_2^{Df}(\rho_{\text{Wei}}^{(N)})$, that is computed in the next section of this paper. The results are scale-invariant and hold for any even N .

by means of a procedure that we name \mathcal{M}_N^3 -fication, involving only LOCC (see Materials and Methods). This immediately implies that, for any $M > \lceil N/2 \rceil$, the multiparticle entanglement E_M^D of ρ can have a nontrivial exact lower bound given by the corresponding multiparticle entanglement of the \mathcal{M}_N^3 state ϖ with the same $\{c_j\}$,

$$E_M^D(\varpi^{\{c_j\}}) \leq E_M^D(\rho), \quad \forall \rho : \text{Tr}(\rho \sigma_j^{\otimes N}) = c_j \quad (j = 1, 2, 3). \quad (4)$$

From a practical point of view, one needs only to measure the three correlation functions $\{c_j\}$, as routinely done in optical, atomic, and spin systems,^{4,44,49,50} to obtain an estimate of the global and partial multiparticle entanglement content of an unknown state ρ , with no need for a full state reconstruction.

Furthermore, the lower bound can be improved if a partial knowledge of the state ρ is assumed, as is usually the case for experiments aiming to produce specific families of states for applications in quantum information processing.^{44,45,49} In those realisations, one typically aims to detect entanglement by constructing optimised entanglement witnesses tailored on the target states.⁴ By exploiting similar ideas, we can optimise the quantitative lower bound in Equation (4) over all possible single-qubit local unitaries applied to the state ρ before the \mathcal{M}_N^3 -fication,

$$\sup_{U_{\otimes}} E_M^D(\varpi^{\{c_j\}}) \leq E_M^D(U_{\otimes} \rho U_{\otimes}^\dagger) = E_M^D(\rho), \quad (5)$$

where $\text{Tr}(U_{\otimes} \rho U_{\otimes}^\dagger \sigma_j^{\otimes N}) = \tilde{c}_j$ and $U_{\otimes} = \otimes_{a=1}^N U^{(a)}$ denote a single-qubit local unitary operation. Experimentally, the optimised bound can then be still accessed by measuring a triple of correlation functions $\{\tilde{c}_j\}$ given by the expectation values of correspondingly rotated Pauli operators on each qubit, $\tilde{c}_j = \langle U_{\otimes}^\dagger \sigma_j^{\otimes N} U_{\otimes} \rangle$, as illustrated in Figure 2a. Optimality in Equation (5) can be achieved by the choice of U_{\otimes} such that $\tilde{h}_{\varpi} = \frac{1}{2} \left(\sum_{j=1}^3 |\tilde{c}_j| - 1 \right)$ is maximum. The optimisation procedure can be significantly simplified when considering a state ρ , which is invariant under permutations of any pair of qubits. In such a case, one may need to optimise only over

three angles $\{\theta, \psi, \phi\}$ parameterising a generic unitary applied to each single qubit; the optimisation can be equivalently performed over an orthogonal matrix acting on the Bloch vector of each qubit (see Materials and Methods).

We can now investigate how useful our results are on concrete examples. Table 3 presents a compendium of optimised analytical lower bounds on the global and partial multiparticle entanglement of several relevant families of N -qubit states,^{46,47,51,52,54–61} up to $N=8$. All the bounds are experimentally accessible by measuring the three correlation functions $\{\tilde{c}_j\}$, corresponding to optimally rotated Pauli operators (Figure 2).

Let us comment on some cases where our analysis is particularly effective. For GHZ states, cluster states, and half-excited Dicke states, which constitute primary resources for quantum computation and metrology,^{37,38} we get the maximum $\tilde{h}_{\varpi} = 1$ for any even N . This means that our bounds remain robust to estimate global and partial entanglement in noisy versions of these states (i.e., when one considers mixtures of any of these states with probability q and the maximally mixed state with probability $1-q$) for all $q > 1/3$. Notably, for values of q sufficiently close to 1, our bounds to global entanglement can be tighter than the (more experimentally demanding) ones derived very recently in ref. 13, as shown in Figure 3a. Focusing on noisy GHZ states, we observe, however, that our scale-invariant threshold $q > 1/3$, obtained by measuring the three canonical Pauli operators for each qubit, is weaker than the well-established inseparability threshold $q > 1/(1+2^{N-1})$.⁹ Nevertheless, we note that our simple quantitative bound given by Equation (4) becomes tight in the paradigmatic limit of pure GHZ states ($q=1$) of any even number N of qubits, thus returning the exact value of their global multiparticle entanglement via Equation (2), despite the fact that such states are not (and are very different from) \mathcal{M}_N^3 states. Equation (4) also provides a useful nonvanishing lower bound to the global (and partial) N -particle entanglement of Wei states in the interval $x \in (\frac{1}{2}, 1]$, for any even N . A comparison between such a bound (with D denoting the relative entropy), which requires only three local measurements, and the true value of the relative

Table 4. Analytical expression of genuine multiparticle entanglement E_2^D for GHZ-diagonal states of any number N of qubits as defined by Equation (6), for representative choices of the distance function D (introduced in Table 2)

Distance D	$g_D(p_{\max})$
Relative entropy D_{RE}	$1 + p_{\max} \log_2 p_{\max} + (1 - p_{\max}) \log_2 (1 - p_{\max})$
Trace D_{Tr}	$p_{\max} - \frac{1}{2}$
Infidelity D_{F}	$\frac{1}{2} - \sqrt{p_{\max}(1 - p_{\max})}$
Squared Bures D_{B}	$2 - \sqrt{2}(\sqrt{1 - p_{\max}} + \sqrt{p_{\max}})$
Squared Hellinger D_{H}	$2 - \sqrt{2}(\sqrt{1 - p_{\max}} + \sqrt{p_{\max}})$

entropy of global N -particle entanglement for these states,⁵⁶ whose experimental evaluation would conventionally require a complete state tomography, is presented in Figure 3b.

Genuine multiparticle entanglement

We now show how general analytical results for geometric measures of genuine multiparticle entanglement can be obtained as well within our approach. The results from the previous section, while quite versatile, cannot provide useful bounds for the complete hierarchy of multiparticle entanglement, because \mathcal{M}_N^3 states are M -separable for all $M \leq \lceil N/2 \rceil$, and thus in particular biseparable for any number N of qubits. Therefore, to investigate genuine entanglement we consider a different reference set of states, specifically formed by mixtures of GHZ states, hence incarnating archetypical representatives of full inseparability.^{5,47} Any such state ξ , which will be referred to as a GHZ-diagonal (in short, \mathcal{G}_N) state, can be written as $\xi = \sum_{i_{\pm}} p_{i_{\pm}} |\beta_{i_{\pm}}^{\pm}\rangle \langle \beta_{i_{\pm}}^{\pm}|$ in terms of its eigenvalues $p_{i_{\pm}}$, with the eigenvectors $|\beta_{i_{\pm}}^{\pm}\rangle = \frac{1}{\sqrt{2}}(\mathbb{I}^{\otimes N} \pm \sigma_1^{\otimes N})|i\rangle$ forming a basis of N -qubit GHZ states (where $\{|i\rangle\}_{i=0}^{2^N-1}$ denotes the binary ordered N -qubit computational basis). The \mathcal{G}_N states have been studied in recent years as testbeds for multiparticle entanglement detection,^{5,48} and specific algebraic measures of genuine multiparticle entanglement such as the N -particle concurrence^{18,21} and negativity¹⁴ have been computed for these states. Here, we calculate exactly the whole class of geometric measures of genuine multiparticle entanglement E_2^D defined by Equation (1), with respect to any contractive and jointly convex distance D , for \mathcal{G}_N states of an arbitrary number N of qubits.

By applying our general framework, we can prove that, for every valid D , the closest biseparable state to any \mathcal{G}_N state can be found within the subset of biseparable \mathcal{G}_N states (see Supplementary Material for detailed derivations). The latter subset is well characterised,⁵ and is formed by all, and only, the \mathcal{G}_N states with eigenvalues such that $p_{\max} \equiv \max_{i_{\pm}} p_{i_{\pm}} \leq 1/2$. We can then show that the closest biseparable \mathcal{G}_N state to an arbitrary \mathcal{G}_N state has maximum eigenvalue equal to $1/2$, which allows us to solve the optimisation in the definition of E_2^D , with respect to every valid D . We have then a closed formula for the geometric multiparticle entanglement of any \mathcal{G}_N state ξ with maximum eigenvalue p_{\max} given by

$$E_2^D(\xi\{p_{i_{\pm}}\}) = \begin{cases} 0, & p_{\max} \leq 1/2; \\ g_D(p_{\max}), & \text{otherwise,} \end{cases} \quad (6)$$

where g_D denotes a monotonically increasing function whose explicit form is specific to each distance D , as reported in Table 4 for typical instances.

Let us comment on some particular results. The genuine multiparticle trace distance of entanglement $E_{2\text{Tr}}^D$ is found to coincide with the genuine multiparticle negativity¹⁴ and with half the genuine multiparticle concurrence¹⁸ for all \mathcal{G}_N states,

thus providing the latter entanglement measures with an insightful geometrical interpretation on this important set of states. Examples of \mathcal{G}_N states include several resources for quantum information processing, such as the noisy GHZ states and Wei states introduced in the previous section. In particular, for noisy GHZ states (described by a pure-state probability q as detailed in Table 3), we recover that every geometric measure of genuine multiparticle entanglement is nonzero if and only if $q > (1 + (1 - 2^N)^{-1})/2 \xrightarrow{N \gg 1} 1/2$ (ref. 5) and monotonically increasing with q , as expected; for $q = 1$ (pure GHZ states), genuine and global entanglement coincide, i.e., the hierarchy of Figure 1 collapses, meaning that all the entanglement of N -qubit GHZ states is genuinely shared among all the N particles.³² On the other hand, the relative entropy of genuine multiparticle entanglement of Wei states^{55,56} can be calculated exactly via Equation (6); interestingly, for even N it is found to coincide with the lower bound to their global entanglement that we had obtained by \mathcal{M}_N^3 -fication, plotted as a solid line in Figure 3b. This means that for these states also the genuine multiparticle entanglement can be quantified entirely by measuring the three canonical correlation functions $\{c_j\}$, for any N . More generally, for arbitrary \mathcal{G}_N states, all the genuine entanglement measures given by equation (6) can be obtained by measuring the maximum GHZ overlap p_{\max} , which requires $N+1$ local measurement settings given explicitly in ref. 48. This is remarkable, as with the same experimental effort needed to detect full inseparability⁵ we have now a complete quantitative picture of genuine entanglement in these states based on any geometric measure, agreeing with and extending the findings of refs 14,18. Furthermore, as evident from Equation (6), all the geometric measures are monotonic functions of each other: our analysis thus reveals that there is a unique ordering of genuinely entangled \mathcal{G}_N states within the distance-based approach of Figure 1.

In the same spirit as the previous section, and in compliance with our general framework, we note that the exact results obtained for the particular reference family of \mathcal{G}_N states provide quantitative lower bounds to the genuine entanglement of general N -qubit states. This follows from the observation that any N -qubit state ρ can be transformed into a \mathcal{G}_N state with eigenvalues $p_{i_{\pm}} = \langle \beta_{i_{\pm}}^{\pm} | \rho | \beta_{i_{\pm}}^{\pm} \rangle$ by an LOCC procedure that we may call GHZ-diagonalisation.¹⁴ Therefore, given a completely general state ρ , one only needs to measure its overlap with a suitable reference GHZ state; if this overlap is found larger than $1/2$, then by using Equation (6) with p_{\max} equal to the measured overlap one obtains analytical lower bounds to the genuine multiparticle entanglement E_2^D of ρ with respect to any desired distance D . As before, the bounds can be optimised in situations of partial prior knowledge—e.g., by applying local unitaries on each qubit before the GHZ-diagonalisation, which has the effect of maximising the overlap with a chosen particular GHZ vector in the basis $\{|\beta_{i_{\pm}}^{\pm}\rangle\}$. The bounds then remain accessible for any state ρ by $N+1$ local measurements,⁴⁸ with exactly the same demand as for just witnessing entanglement.⁵

For instance, for the singlet state $|\Psi^{(4)}\rangle$,⁶² which is a relevant resource in a number of quantum protocols including multiuser secret sharing,^{63–65} one has $p_{\max} = \langle \beta_3^+ | \Psi^{(4)} \rangle \langle \Psi^{(4)} | \beta_3^+ \rangle = 2/3 > 1/2$, obtainable by measuring the overlap with the GHZ basis state $|\beta_3^+\rangle = (|0011\rangle + |1100\rangle)/\sqrt{2}$. Optimised bounds to the genuine multiparticle entanglement of half-excited Dicke states $|D_{N/2}^{(N)}\rangle$ (for even $N \geq 4$), defined in Table 3,^{58,66} can be found as well based on GHZ-diagonalisation, and are expressed by $p_{\max}^{(N)} = \binom{N}{N/2} 2^{1-N}$, meaning that they become looser with increasing N and stay nonzero only up to $N=8$. In this respect, we note that alternative methods to detect full inseparability of Dicke states for any N are

Table 5. Accessible lower bounds to global, partial and genuine multiparticle entanglement for a variety of experimental quantum states

a						Global and partial multiparticle entanglement
State	Reference	Fidelity (%)	$\{\bar{c}_1, \bar{c}_2, \bar{c}_3\}$		$\sum_{j=1}^3 \bar{c}_j $	$E_M^{D_{tr}}$
$\rho_S^{(4)}$	44	96.83 ± 0.05	$\{0.401 \pm 0.004, 0.362 \pm 0.004, 0.397 \pm 0.008\}$		1.16 ± 0.01	0.040 ± 0.002
$\rho_{D_3}^{(6)}$	51	56 ± 2	$\{0.8 \pm 0.2, 0.5 \pm 0.2, -0.3 \pm 0.1\}$		1.6 ± 0.3	0.15 ± 0.08
$\rho_{D_3}^{(6)}$	52	65 ± 2	$\{0.63 \pm 0.02, 0.63 \pm 0.02, -0.42 \pm 0.02\}$		1.69 ± 0.04	0.17 ± 0.01
$\rho_{GHZ}^{(3)}$	67	87.9	$\{-0.497, 0.515, -0.341\}$		1.35	0.102
$\rho_{GHZ}^{(4)}$	67	80.3	$\{0.663, 0.683, 0.901\}$		2.25	0.312
$\rho_{W_A}^{(4)}$	67	19.4	$\{-0.404, 0.454, -0.378\}$		1.24	0.0589
$\rho_{W_B}^{(4)}$	67	31.4	$\{0.472, -0.468, -0.446\}$		1.39	0.0963
b						Genuine multiparticle entanglement
State	Reference	Fidelity (%)	$E_2^{D_{re}}$	$E_2^{D_{tr}}$	$E_2^{D_{tr}}$	$E_2^{D_b}$
$\rho_{GHZ}^{(3)}$	50	97.0 ± 0.3	0.81 ± 0.02	0.470 ± 0.003	0.329 ± 0.008	0.36 ± 0.01
$\rho_{GHZ}^{(4)}$	50	95.7 ± 0.3	0.74 ± 0.01	0.457 ± 0.003	0.297 ± 0.007	0.323 ± 0.008
$\rho_{GHZ}^{(5)}$	50	94.4 ± 0.5	0.69 ± 0.02	0.444 ± 0.005	0.27 ± 0.01	0.29 ± 0.01
$\rho_{GHZ}^{(6)}$	50	89.2 ± 0.4	0.51 ± 0.01	0.392 ± 0.004	0.190 ± 0.005	0.200 ± 0.006
$\rho_{GHZ}^{(8)}$	50	81.7 ± 0.4	0.313 ± 0.009	0.317 ± 0.004	0.113 ± 0.003	0.117 ± 0.003
$\rho_{GHZ}^{(10)}$	50	62.6 ± 0.6	0.046 ± 0.004	0.126 ± 0.006	0.016 ± 0.002	0.016 ± 0.002
$\rho_{GHZ}^{(14)}$	50	50.8 ± 0.9	0.0002 ± 0.0004	0.008 ± 0.009	0.0001 ± 0.0001	0.0001 ± 0.0001

(a) Accessible lower bounds to global and partial multiparticle entanglement of some experimentally prepared states, given by Equation (5) and evaluated in particular for the trace distance of entanglement $E^{D_{tr}}$ by using Equation (2) for even N and Equation (3) for odd N . Following the theoretical analysis of Table 3, data obtained by direct measurements of the canonical correlation functions were used to construct bounds for a noisy Smolin state of 4 photons,⁴⁴ noisy Dicke states of 6 photons^{51,52} and noisy GHZ states of four ions.⁶⁷ For noisy GHZ states of three ions and noisy W states of four ions (two implementations labelled as A and B),⁶⁷ full data sets were used to extract the optimised correlation functions $\{\bar{c}_j\}$ required for the bounds. For all the presented experimental states (whose fidelities with the ideal target states are reported for reference), we are able to provide a reliable estimate of the multiparticle entanglement E_M^D for any $M > \lfloor N/2 \rfloor$. (b) Lower bounds to genuine multiparticle entanglement of experimental noisy GHZ states of up to 14 ions,⁵⁰ as quantified in terms of all the distance-based entanglement measures E_2^D reported in Table 4, obtained by Equation (6) with p_{\max} given in each case by the measured fidelity with the pure reference GHZ state. All the reported entanglement estimates are obtained from the same data needed to witness full inseparability, which for general N -qubit states can be accessed by $N+1$ local measurements without the need for a full tomography.

available,^{4,51,52} but quantitative results are lacking in general. Nevertheless, applying our general approach to an alternative reference family more tailored to the Dicke states could yield tighter lower bounds that do not vanish beyond $N=8$.

Finally, notice that a lower bound to a distance-based measure of genuine multiparticle entanglement, as derived in this section, is automatically also a lower bound to corresponding measures of global and any form of partial entanglement, as evident by looking at the geometric picture in Figure 1. However, for states that are entangled yet not genuinely entangled, the simple bound from the previous section remains instrumental to assess their inseparability with minimum effort. \mathcal{M}_N^3 states are themselves instances of such states (in fact, for even N , \mathcal{M}_N^3 states are also \mathcal{G}_N states, but with $p_{\max} \leq 1/2$ for $N > 2$).

Applications to experimental states

In this section, we benchmark the applicability of our results to real data from recent experiments.^{44,49–52,67}

In refs 44,45 the authors used quantum optical setups to prepare an instance of a bound entangled four-qubit state, known as Smolin state.⁶⁸ Such a state cannot be written as a convex mixture of product states of the four qubits, yet no entanglement can be distilled out of it, thus incarnating the irreversibility in entanglement manipulation, while still representing a useful resource for information locking and quantum secret sharing.^{3,46} It turns out that noisy Smolin states are particular types of \mathcal{M}_N^3 states (for any even N),^{43,46} that in the representation of Figure 2b

are located along the segment connecting the tetrahedron vertex $\{(-1)^{N/2}, (-1)^{N/2}, (-1)^{N/2}\}$ with the origin. Therefore, this work provides exact analytical formulae for all the nontrivial hierarchy of their global and partial entanglement, as mentioned in Table 3. In the specific experimental implementation of ref. 44 for $N=4$, the global entanglement was detected (but not quantified) via a witness constructed by measuring precisely the three correlation functions $\{c_j\}$. On the basis of the existing data alone (and without assuming that the produced state is within the \mathcal{M}_N^3 family), we can then provide a quantitative estimate to the multiparticle entanglement of this experimental bound entangled state in terms of any geometric measure E_M^D , by using Table 2. The results are reported in Table 5a for the illustrative case of the trace distance.

Remaining within the domain of quantum optics, recently two laboratories reported the creation of six-photon Dicke states $|D_3^{(6)}\rangle$.^{51,52} Dicke states⁵⁸ are valuable resources for quantum metrology, computation and networked communication and emerge naturally in many-body systems as ground states of the isotropic Lipkin–Meshkov–Glick model.⁶⁶ On the basis of the values of the three correlation functions $\{c_j\}$, which were measured in refs 51,52 to construct some entanglement witnesses, we can provide quantitative bounds to their global and partial geometric entanglement E_M^D (for $4 \leq M \leq 6$) from Equation (4); see Table 5a.

A series of experiments at Innsbruck^{40,49,50,67} resulted in the generation of a variety of relevant multi-qubit states with trapped ion setups, for explorations of fundamental science and for the

implementation of quantum protocols. In those realisations, data acquisition and processing for the purpose of entanglement verification was often a more demanding task than running the experiment itself.⁴⁹ Focusing first on global and partial entanglement, we obtained full datasets for experimental density matrices corresponding to particularly noisy GHZ and W states of up to four qubits, produced during laboratory test runs.⁶⁷ Despite the relatively low fidelity with their ideal target states, we still obtain meaningful quantitative bounds from Equation (5). The results are compactly presented in Table 5a.

Regarding now genuine multiparticle entanglement, the authors of ref. 50 reported the creation of (noisy) GHZ states of up to $N = 14$ trapped ions. In each of these states, full inseparability was witnessed by measuring precisely the maximum overlap p_{\max} with a reference pure GHZ state, without the need for complete state tomography. Thanks to Equation (6), we can now use the same data to obtain a full quantification of the genuine N -particle entanglement of these realistic states, according to any measure E_M^D , at no extra cost in terms of experimental or computational resources. The results are in Table 5b, for all the representative choices of distances enumerated in Table 4. Notice that we do not need to assume that the experimentally produced states are in the \mathcal{G}_N set: the obtained results can be still safely regarded as lower bounds.

DISCUSSION

We have introduced a general framework for estimating and quantifying geometric entanglement monotones. This enabled us to achieve a compendium of exact results on the quantification of general distance-based measures of (global, partial and genuine) multiparticle entanglement in some pivotal reference families of N -qubit mixed states. In turn, these results allowed us to establish faithful lower bounds to various forms of multiparticle entanglement for arbitrary states, accessible by few local measurements and effective on prominent resource states for quantum information processing.

Our results can be regarded as realising simple yet particularly convenient instances of quantitative entanglement witnesses,^{22,23} with the crucial advance that our lower bounds are analytical (in contrast to conventional numerical approaches requiring semidefinite programming) and hold for all valid geometric measures of entanglement, which are endowed with meaningful operational interpretations yet have been traditionally hard to evaluate.^{13,69}

A key aspect of our analysis lies in fact in the generality of the adopted techniques, which rely on natural information-theoretic requirements of contractivity and joint convexity of any valid distance D entering Equation (1). We can expect our general framework to be applicable to other reference families of states (for example, states diagonal in a basis of cluster states,^{14,69} or more general states with X-shaped density matrices¹⁸), thereby leading to alternative entanglement bounds for arbitrary states, which might be more tailored to different classes, or to specific measurement settings in laboratory.

Furthermore, our framework lends itself to numerous other applications. These include the obtention of accessible analytical results for the geometric quantification of other useful forms of multiparticle quantum correlations, such as Einstein–Podolsky–Rosen steering,^{70,71} and Bell nonlocality in many-body systems.⁶⁶ This can eventually lead to a unifying characterisation, resting on the structure of information geometry, of the whole spectrum of genuine signatures of quantumness in cooperative phenomena. We plan to extend our approach in this sense in subsequent works.

Another key feature of our results is the experimental accessibility. Having tested our entanglement bounds on a selection of very different families of theoretical and

experimentally produced states with high levels of noise, we can certify their usefulness in realistic scenarios. We recall that, for instance, three canonical local measurements suffice to quantify exactly the global entanglement of GHZ states of any even number N of qubits, whereas $N+1$ local measurements provide their exact genuine entanglement, according to every geometric measure for any N , when such states are realistically mixed with white noise. Compared with other complementary studies of accessible quantification of multiparticle entanglement,^{13–23} our study retains not only a comparably low resource demand but also crucial aspects such as efficiency and versatility, as shown in Table 1. This can lead to a considerable simplification of quantitative resource assessment in future experiments based on large-scale entangled registers, involving e.g., two quantum bytes (16 qubits) and beyond.^{50,67}

MATERIALS AND METHODS

Distance-based measures of multiparticle entanglement

A general distance-based measure of multiparticle entanglement E_M^D is defined in Equation (1). In this work, the distance D is required to satisfy the following two physical constraints:

(D.i) Contractivity under quantum channels, i.e., $D(\Omega(\rho), \Omega(\rho')) \leq D(\rho, \rho')$, for any states ρ, ρ' , and any completely positive trace preserving map Ω ;

(D.ii) Joint convexity, i.e., $D(q\rho + (1-q)\rho', q\chi + (1-q)\chi') \leq qD(\rho, \chi) + (1-q)D(\rho', \chi')$, for any states ρ, ρ', χ , and χ' , and any $q \in [0, 1]$.

Constraint (D.i) implies that E_M^D is invariant under local unitaries and monotonically nonincreasing under LOCC (i.e., it is an entanglement monotone²⁴). Constraint (D.ii) implies that E_M^D is also convex. A selection of distance functionals with respect to these properties is given in Table 2.

\mathcal{M}_N^3 -fication Theorem. Any N -qubit state ρ can be transformed into a corresponding \mathcal{M}_N^3 state ϖ through a fixed transformation, Θ , consisting of single-qubit LOCC, such that $\Theta(\rho) = \varpi = \frac{1}{2^N}(\mathbb{I}^{\otimes N} + \sum_{i=1}^N c_i \sigma_i^{\otimes N})$, where $c_i = \text{Tr}(\rho \sigma_i^{\otimes N})$.

Proof. Here we sketch the form of the \mathcal{M}_N^3 -fication channel Θ . We begin by setting $2(N-1)$ single-qubit local unitaries $\{U_j\}_{j=1}^{2(N-1)} = \{(\sigma_1 \otimes \sigma_1 \otimes \mathbb{I}^{\otimes N-2}), (\mathbb{I} \otimes \sigma_1 \otimes \sigma_1 \otimes \mathbb{I}^{\otimes N-3}), \dots, (\mathbb{I}^{\otimes N-3} \otimes \sigma_1 \otimes \sigma_1 \otimes \mathbb{I}), (\mathbb{I}^{\otimes N-2} \otimes \sigma_1 \otimes \sigma_1), (\sigma_2 \otimes \sigma_2 \otimes \mathbb{I}^{\otimes N-2}), (\mathbb{I} \otimes \sigma_2 \otimes \sigma_2 \otimes \mathbb{I}^{\otimes N-3}), \dots, (\mathbb{I}^{\otimes N-3} \otimes \sigma_2 \otimes \sigma_2 \otimes \mathbb{I}), (\mathbb{I}^{\otimes N-2} \otimes \sigma_2 \otimes \sigma_2)\}$. Then, we fix a sequence of states $\{\rho_0, \rho_1, \dots, \rho_{2(N-1)}\}$ defined by $\rho_j = \frac{1}{2}(\rho_{j-1} + U_j \rho_{j-1} U_j^\dagger)$, for $j \in \{1, 2, \dots, 2(N-1)\}$. By setting $\rho_0 = \rho$ and $\rho_{2(N-1)} = \Theta(\rho)$, we define the required channel: $\Theta(\rho) = \frac{1}{2^{2(N-1)}} \sum_{i=1}^{2^{2(N-1)}} U_i \rho U_i^\dagger$, where: $\{U_i\}_{i=1}^{2^{2(N-1)}} = \left\{ \mathbb{I}^{\otimes N}, \{U_i\}_{i=1}^{2(N-1)}, \{U_{i_2} U_{i_1}\}_{i_2 > i_1=1}^{2(N-1)}, \dots, \{U_{i_{2(N-1)}} \dots U_{i_2} U_{i_1}\}_{i_{2(N-1)} > \dots > i_2 > i_1=1}^{2(N-1)} \right\}$. Notice that $\{U_i\}_{i=1}^{2^{2(N-1)}}$

is still a sequence of single-qubit local unitaries. Since Θ is a convex mixture of such local unitaries, it belongs to the class of single-qubit LOCC, mapping any M -separable set into itself. In the Supplementary Material, we show that $\Theta(\rho) = \varpi$, concluding the proof.

Lower-bound optimisation

For any valid distance-based measure of global and partial multiparticle entanglement E_M^D , the maximisation in Equation (5) is equivalent (for even N) to maximising $|\tilde{c}_1| + |\tilde{c}_2| + |\tilde{c}_3|$, where $\tilde{c}_j = \text{Tr}[U_{\otimes} \rho U_{\otimes}^\dagger \sigma_j^{\otimes N}]$, over local single-qubit unitaries $U_{\otimes} = \bigotimes_{\alpha} U^{(\alpha)}$ ($\alpha = 1, \dots, N$). By using the well-known correspondence between the special unitary group $\text{SU}(2)$ and special orthogonal group $\text{SO}(3)$, we have that to any one-qubit unitary $U^{(\alpha)}$ corresponds the orthogonal 3×3 matrix $O^{(\alpha)}$ such that $U^{(\alpha)} \vec{n} \cdot \vec{\sigma} U^{(\alpha)\dagger} = (O^{(\alpha)} \vec{n}) \cdot \vec{\sigma}$, where $\vec{n} = \{n_1, n_2, n_3\} \in \mathbb{R}^3$ and $\vec{\sigma} = \{\sigma_1, \sigma_2, \sigma_3\}$ is the vector of Pauli matrices. We have then that $\sup_{\{U^{(\alpha)}\}} (|\tilde{c}_1| + |\tilde{c}_2| + |\tilde{c}_3|) = \sup_{\{O^{(\alpha)}\}} (|\tilde{T}_{11\dots 1}| + |\tilde{T}_{22\dots 2}| + |\tilde{T}_{33\dots 3}|)$, where $\tilde{T}_{i_1 i_2 \dots i_N} = \sum_{j_1 j_2 \dots j_N} T_{j_1 j_2 \dots j_N} O_{i_1 j_1}^{(1)} O_{i_2 j_2}^{(2)} \dots O_{i_N j_N}^{(N)}$, and $T_{i_1 i_2 \dots i_N} = \text{Tr}[\rho(\sigma_{i_1} \otimes \sigma_{i_2} \otimes \dots \otimes \sigma_{i_N})]$. In the case of permutationally invariant states ρ , the $3 \times 3 \times \dots \times 3$ tensor $T_{i_1 i_2 \dots i_N}$ is fully symmetric, i.e., $T_{i_1 i_2 \dots i_N} = T_{\vartheta(i_1 i_2 \dots i_N)}$ for any permutation ϑ of the indices, so that the optimisation can be achieved

when $O^{(1)} = O^{(2)} = \dots = O^{(N)}$ (ref. 72). As indicated in the main text, we then need to perform the maximisation over just the three angles $\{\theta, \psi, \phi\}$, which determine the orthogonal matrix $O^{(a)}$ corresponding to an arbitrary single-qubit unitary

$$U^{(a)} = \begin{pmatrix} \cos \frac{\theta}{2} e^{-i\frac{\phi+\psi}{2}} & -i \sin \frac{\theta}{2} e^{-i\frac{\phi-\psi}{2}} \\ -i \sin \frac{\theta}{2} e^{i\frac{\phi-\psi}{2}} & \cos \frac{\theta}{2} e^{i\frac{\phi+\psi}{2}} \end{pmatrix}.$$

As a special case, for a two-qubit state ($N=2$) the optimal local operation is the one which diagonalises the correlation matrix ($T_{i_1 i_2}$).

ACKNOWLEDGEMENTS

We warmly thank Thomas Monz, Mauro Paternostro, Christian Schwemmer and Witłef Wieczorek for providing experimental data, and we acknowledge fruitful discussions with (in alphabetical order) I Almeida Silva, M Blasone, D Cavalcanti, E Carnio, T Chanda, M Christandl, P Comon, M Cramer, M Gessner, T Ginestra, D Gross, O Gühne, M Guta, M Huber, F Illuminati, I Kogias, T Kyraios, P Liuzzo-Scorpo, C Macchiavello, A Milne, T Monz, P Ott, AK Pal, M Piani, M Prater, S Rat, A Sanpera, P Skrzypczyk, A Streltsov, G Tóth and A. Winter. This work was supported by the European Research Council (ERC) Starting Grant GQCOP, Grant Agreement No. 637352.

CONTRIBUTIONS

All the authors conceived the idea, derived the technical results, discussed all stages of the project, and prepared the manuscript and figures.

COMPETING INTERESTS

The authors declare no conflict of interest.

REFERENCES

- Einstein, A., Podolsky, B. & Rosen, N. Can quantum-mechanical description of physical reality be considered complete? *Phys. Rev.* **47**, 777–780 (1935).
- Vedral, V. Quantum entanglement. *Nat. Phys.* **10**, 256–258 (2014).
- Horodecki, R., Horodecki, P., Horodecki, M. & Horodecki, K. Quantum entanglement. *Rev. Mod. Phys.* **81**, 865–942 (2009).
- Gühne, O. & Tóth, G. Entanglement detection. *Phys. Rep.* **474**, 1–75 (2009).
- Gühne, O. & Seevinck, M. Separability criteria for genuine multiparticle entanglement. *New J. Phys.* **12**, 053002 (2010).
- Gao, T., Yan, F. & van Enk, S. J. Permutationally invariant part of a density matrix and nonseparability of n -qubit states. *Phys. Rev. Lett.* **112**, 180501 (2014).
- Levi, F. & Mintert, F. Hierarchies of multipartite entanglement. *Phys. Rev. Lett.* **110**, 150402 (2013).
- Huber, M., Mintert, F., Gabriel, A. & Hiesmayr, B. C. Detection of high-dimensional genuine multipartite entanglement of mixed states. *Phys. Rev. Lett.* **104**, 215001 (2010).
- Dür, W. & Cirac, J. I. Classification of multiqubit mixed states: Separability and distillability properties. *Phys. Rev. A* **61**, 042314 (2000).
- Gabriel, A., Hiesmayr, B. C. & Huber, M. Criterion for k -separability in mixed multipartite systems. *Quant. Inform. Comput.* **10**, 829–836 (2010).
- Klöckl, C. & Huber, M. Characterizing multipartite entanglement without shared reference frames. *Phys. Rev. A* **91**, 042339 (2015).
- Badziąg, P., Brukner, Č., Laskowski, W., Paterek, T. & Żukowski, M. Experimentally friendly geometrical criteria for entanglement. *Phys. Rev. Lett.* **100**, 140403 (2008).
- Buchholz, L. E., Moroder, T. & Gühne, O. Evaluating the geometric measure of multiparticle entanglement. *Ann. Phys. (Berlin)* **528**, 278–287 (2016).
- Hofmann, M., Moroder, T. & Gühne, O. Analytical characterization of the genuine multiparticle negativity. *J. Phys. A: Math. Theor.* **47**, 155301 (2014).
- Siewert, J. & Eltschka, C. Quantifying tripartite entanglement of three-qubit generalized werner states. *Phys. Rev. Lett.* **108**, 230502 (2012).
- Eltchka, C. & Siewert, J. A quantitative witness for greenberger-horne-zeilinger entanglement. *Sci. Rep.* **2** (2012).
- Wu, J.-Y., Kampermann, H., Bruß, D., Klöckl, C. & Huber, M. Determining lower bounds on a measure of multipartite entanglement from few local observables. *Phys. Rev. A* **86**, 022319 (2012).
- Hashemi Rafsanjani, S. M., Huber, M., Broadbent, C. J. & Eberly, J. H. Genuinely multipartite concurrence of n -qubit x matrices. *Phys. Rev. A* **86**, 062303 (2012).
- Audenaert, K. & Plenio, M. When are correlations quantum?—verification and quantification of entanglement by simple measurements. *New J. Phys.* **8**, 266 (2006).
- Wunderlich, H. & Plenio, M. B. Quantitative verification of entanglement and fidelities from incomplete measurement data. *J. Mod. Optics* **56**, 2100–2105 (2009).
- Ma, Z.-H. et al. Measure of genuine multipartite entanglement with computable lower bounds. *Phys. Rev. A* **83**, 062325 (2011).
- Gühne, O., Reimpell, M. & Werner, R. F. Estimating entanglement measures in experiments. *Phys. Rev. Lett.* **98**, 110502 (2007).
- Eisert, J., Brandão, F. G. & Audenaert, K. M. Quantitative entanglement witnesses. *New J. Phys.* **9**, 46 (2007).
- Plenio, M. B. & Virmani, S. An introduction to entanglement measures. *Quant. Inf. Comput.* **7**, 1 (2007).
- Sarovar, M., Ishizaki, A., Fleming, G. R. & Whaley, K. B. Quantum entanglement in photosynthetic light-harvesting complexes. *Nat. Phys.* **6**, 462–467 (2010).
- Cramer, M., Plenio, M. B. & Wunderlich, H. Measuring entanglement in condensed matter systems. *Phys. Rev. Lett.* **106**, 020401 (2011).
- Cramer, M. et al. Spatial entanglement of bosons in optical lattices. *Nat. Commun.* **4**, 2161 (2013).
- Marty, O. et al. Quantifying entanglement with scattering experiments. *Phys. Rev. B* **89**, 125117 (2014).
- Marty, O., Cramer, M. & Plenio, M. B. Practical entanglement estimation for spin-system quantum simulators. *Phys. Rev. Lett.* **116**, 105301 (2016).
- Vedral, V., Plenio, M. B., Rippin, M. A. & Knight, P. L. Quantifying entanglement. *Phys. Rev. Lett.* **78**, 2275–2279 (1997).
- Wei, T.-C. & Goldbart, P. M. Geometric measure of entanglement and applications to bipartite and multipartite quantum states. *Phys. Rev. A* **68**, 042307 (2003).
- Blasone, M., Dell'Anno, F., De Siena, S. & Illuminati, F. Hierarchies of geometric entanglement. *Phys. Rev. A* **77**, 062304 (2008).
- Bengtsson, I. & Życzkowski, K. *Geometry of Quantum States: An Introduction to Quantum Entanglement* (Cambridge Univ. Press, 2006).
- Wei, T.-C., Das, D., Mukhopadhyay, S., Vishveshwara, S. & Goldbart, P. M. Global entanglement and quantum criticality in spin chains. *Phys. Rev. A* **71**, 060305 (2005).
- Bihm, O., Nielsen, M. A. & Osborne, T. J. Entanglement monotone derived from grover's algorithm. *Phys. Rev. A* **65**, 062312 (2002).
- Bell, B. A. et al. Experimental demonstration of graph-state quantum secret sharing. *Nat. Commun.* **5**, 5480 (2014).
- Giovannetti, V., Lloyd, S. & Maccone, L. Advances in quantum metrology. *Nat. Photon.* **5**, 222 (2011).
- Briegel, H. J., Browne, D. E., Dür, W., Raussendorf, R. & den Nest, M. V. *Nat. Phys.* **5**, 19–26 (2009).
- Tiersch, M., Popescu, S. & Briegel, H. J. A critical view on transport and entanglement in models of photosynthesis. *Phil. Trans. Roy. Soc. A* **370**, 3771–3786 (2012).
- Barreiro, J. T. et al. Experimental multiparticle entanglement dynamics induced by decoherence. *Nat. Phys.* **6**, 943 (2010).
- Hayashi, M., Markham, D., Murao, M., Owari, M. & Virmani, S. Bounds on multipartite entangled orthogonal state discrimination using local operations and classical communication. *Phys. Rev. Lett.* **96**, 040501 (2006).
- Streltsov, A., Kampermann, H. & Bruß, D. Linking a distance measure of entanglement to its convex roof. *New J. Phys.* **12**, 123004 (2010).
- Hiesmayr, B. C., Hipp, F., Huber, M., Krammer, P. & Spengler, C. Simplex of bound entangled multipartite qubit states. *Phys. Rev. A* **78**, 042327 (2008).
- Lavoie, J., Kaltenbaek, R., Piani, M. & Resch, K. J. Experimental bound entanglement in a four-photon state. *Phys. Rev. Lett.* **105**, 130501 (2010).
- Amselem, E. & Bourennane, M. Experimental four-qubit bound entanglement. *Nat. Phys.* **5**, 748 (2009).
- Augusiak, R. & Horodecki, P. Generalized smolin states and their properties. *Physical Review A* **73**, 012318 (2006).
- Greenberger, D. M., Horne, M. & Zeilinger, A. in *Bell's Theorem, Quantum Theory, and Conceptions of the Universe* (ed. Kafatos, M.) 69–72 (Kluwer, 1989).
- Gühne, O., Lu, C.-Y., Gao, W.-B. & Pan, J.-W. Toolbox for entanglement detection and fidelity estimation. *Phys. Rev. A* **76**, 030305 (2007).
- Häffner, H. et al. Scalable multiparticle entanglement of trapped ions. *Nature* **438**, 643–646 (2005).
- Monz, T. et al. 14-qubit entanglement: creation and coherence. *Phys. Rev. Lett.* **106**, 130506 (2011).
- Prevedel, R. et al. Experimental realization of dicke states of up to six qubits for multiparty quantum networking. *Phys. Rev. Lett.* **103**, 020503 (2009).
- Wieczorek, W. et al. Experimental entanglement of a six-photon symmetric dicke state. *Phys. Rev. Lett.* **103**, 020504 (2009).
- Carnio, E. G., Buchleitner, A. & Gessner, M. Robust asymptotic entanglement under multipartite collective dephasing. *Phys. Rev. Lett.* **115**, 010404 (2015).

54. Dür, W., Vidal, G. & Cirac, J. I. Three qubits can be entangled in two inequivalent ways. *Phys. Rev. A* **62**, 062314 (2000).
55. Wei, T. C., Altepeter, J. B., Goldbart, P. M. & Munro, W. J. Measures of entanglement in multipartite bound entangled states. *Phys. Rev. A* **70**, 022322 (2004).
56. Wei, T.-C. Relative entropy of entanglement for multipartite mixed states: Permutation-invariant states and dür states. *Phys. Rev. A* **78**, 012327 (2008).
57. Raussendorf, R. & Briegel, H. J. A one-way quantum computer. *Phys. Rev. Lett.* **86**, 5188–5191 (2001).
58. Dicke, R. H. Coherence in spontaneous radiation processes. *Phys. Rev.* **93**, 99–110 (1954).
59. Cabello, A. Solving the liar detection problem using the four-qubit singlet state. *Phys. Rev. A* **68**, 012304 (2003).
60. Kiesel, N. *et al.* Experimental analysis of a four-qubit photon cluster state. *Phys. Rev. Lett.* **95**, 210502 (2005).
61. Kiesel, N., Schmid, C., Tóth, G., Solano, E. & Weinfurter, H. Experimental observation of four-photon entangled dicke state with high fidelity. *Phys. Rev. Lett.* **98**, 063604 (2007).
62. Weinfurter, H. & Żukowski, M. Four-photon entanglement from down-conversion. *Phys. Rev. A* **64**, 010102 (2001).
63. Bourennane, M. *et al.* Decoherence-free quantum information processing with four-photon entangled states. *Phys. Rev. Lett.* **92**, 107901 (2004).
64. Murao, M., Jonathan, D., Plenio, M. & Vedral, V. Quantum telecloning and multiparticle entanglement. *Phys. Rev. A* **59**, 156 (1999).
65. Gaertner, S., Kurtsiefer, C., Bourennane, M. & Weinfurter, H. Experimental demonstration of four-party quantum secret sharing. *Phys. Rev. Lett.* **98**, 020503 (2007).
66. Tura, J. *et al.* Detecting nonlocality in many-body quantum states. *Science* **344**, 1256–1258 (2014).
67. Monz, T. *Quantum information processing beyond ten ion-qubits*, Ph.D. thesis Institute for Experimental Physics, University of Innsbruck, (2011).
68. Smolin, J. A. Four-party unlockable bound entangled state. *Phys. Rev. A* **63**, 032306 (2001).
69. Chen, X.-Y., Yu, P., Jiang, L.-Z. & Tian, M. Genuine entanglement of four-qubit cluster diagonal states. *Phys. Rev. A* **87**, 012322 (2013).
70. Wiseman, H. M., Jones, S. J. & Doherty, A. C. Steering, entanglement, nonlocality, and the einstein-podolsky-rosen paradox. *Phys. Rev. Lett.* **98**, 140402 (2007).
71. Armstrong, S. *et al.* Multipartite einstein-podolsky-rosen steering and genuine tripartite entanglement with optical networks. *Nat. Phys.* **11**, 167 (2015).
72. Comon, P. & Sorensen, M. Tensor diagonalization by orthogonal transforms. Report ISRN I3S-RR-2007-06-FR (2007). Available online (<http://www.i3s.unice.fr/~mh/RR/2007/RR-07.06-P.COMON.pdf>).



This work is licensed under a Creative Commons Attribution 4.0 International License. The images or other third party material in this article are included in the article's Creative Commons license, unless indicated otherwise in the credit line; if the material is not included under the Creative Commons license, users will need to obtain permission from the license holder to reproduce the material. To view a copy of this license, visit <http://creativecommons.org/licenses/by/4.0/>

© The Author(s) 2016

Supplementary Information accompanies the paper on the *npj Quantum Information* website (<http://www.nature.com/npjqi>)